Article

Cell Reports

Phages Mediate Bacterial Self-Recognition

Graphical Abstract

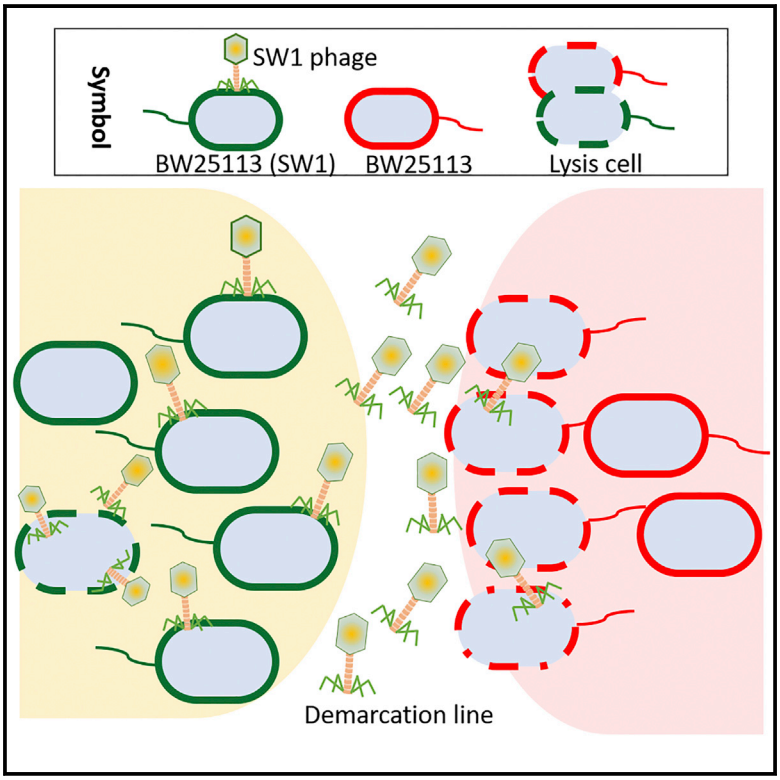

Highlights

- Swimming bacteria distinguish rivals through the T1-type lytic phage SW1
- Phage SW1 relies on the cryptic prophage protein YfdM to replicate
- Cells infected with SW1 outcompete rivals during foraging and phage challenge
- Self-recognition is also seen for cells with lysogenic phages ϕ80 and lambda

Authors

Sooyeon Song, Yunxue Guo, Jun-Seob Kim, Xiaoxue Wang, Thomas K. Wood

Correspondence

xxwang@scsio.ac.cn (X.W.), twood@engr.psu.edu (T.K.W.)

In Brief

While bacteria are foraging, it is beneficial for them to distinguish themselves from related strains. Here, Song et al. show that a lytic phage that infects *Escherichia coli* may be used to preferentially lyse cells that are not infected so that the infected cells outcompete their virus-free rivals.

Song et al., 2019, Cell Reports *27*, 737–749
April 16, 2019
https://doi.org/10.1016/j.celrep.2019.03.070

CellPress

Cell Reports
Article

Phages Mediate Bacterial Self-Recognition

Sooyeon Song,[1] Yunxue Guo,[2] Jun-Seob Kim,[3] Xiaoxue Wang,[2,*] and Thomas K. Wood[1,4,*]
[1]Department of Chemical Engineering, Pennsylvania State University, University Park, PA 16802-4400, USA
[2]CAS Key Laboratory of Tropical Marine Bio-resources and Ecology, South China Sea Institute of Oceanology, Chinese Academy of Sciences, Guangzhou 510301, China
[3]Infectious Disease Research Center, Korea Research Institute of Bioscience and Biotechnology, Daejeon 34141, South Korea
[4]Lead Contact
*Correspondence: xxwang@scsio.ac.cn (X.W.), twood@engr.psu.edu (T.K.W.)
https://doi.org/10.1016/j.celrep.2019.03.070

SUMMARY

Cells are social, and self-recognition is a conserved aspect of group behavior where cells assist kin and antagonize non-kin. However, the role of phage in self-recognition is unexplored. Here we find that a demarcation line is formed between different swimming *Escherichia coli* strains but not between identical clones; hence, motile cells discriminate between self and non-self. The basis for this self-recognition is a 49 kb, T1-type, lytic phage of the family Siphoviridae (named here SW1) that controls formation of the demarcation line by utilizing one of the host's cryptic prophage proteins, YfdM of CPS-53, to propagate. Critically, SW1 provides a conditional benefit to *E. coli* K-12 compared with the identical strain that lacks the phage. A demarcation line is also formed when strains harbor either the lysogenic phage ϕ80 or lambda and encounter siblings that lack the lysogen. In summary, bacteria can use phage to distinguish siblings that lack phage.

INTRODUCTION

Cellular motility impacts bacterial physiology by providing a means for acquiring nutrients (e.g., chemotaxis) (Armitage, 1992), evading stress (Armitage, 1992), initiating biofilm formation (Wood et al., 2006), and dispersing biofilms (Petrova and Sauer, 2016). Two of the best-studied forms of motility are swarming, which is flagella-based movement *on top* of a solid surface, and swimming, which is flagella-based movement *through* liquids (Alberti and Harshey, 1990). Motility can also be social and is a critical part of self-recognition, a behavior that impacts nourishment, virulence, iron acquisition, protection, quorum sensing, biofilm formation, and fruiting bodies (Strassmann et al., 2011). In effect, self-recognition allows bacteria to form social groups (Wall, 2016).

Self-recognition mechanisms studied to date depend on surface receptors and diffusible chemical signals (Troselj et al., 2018). For example, during the swarming of *Proteus mirabilis,* self-recognition takes the form of a demarcation line (Dienes line; Gibbs et al., 2008); as cells move on the surface, a visible gap is formed between different strains due to killing as a result of cell-cell contact through identity proteins (IdsD and IdsE) that are probably delivered by a type VI secretion system (Cardarelli et al., 2015) as well as due to killing by bacteriocins (Kusek and Herman, 1980). Similarly, several self-recognition determinants have been identified for swarming *Bacillus subtilis* cells, including contact-dependent inhibition and secreted antimicrobials (Lyons et al., 2016). Additionally, self-recognition during swarming is mediated through a toxin-antitoxin system requiring outer membrane exchange in *Myxococcus xanthus*, in which non-motile cells can prevent the swarming of cells that lack the antitoxin (Dey et al., 2016). However, self-recognition during swimming motility (i.e., motility *through* liquids) has not been reported previously, and self-recognition during swimming or swarming has not been linked to phage-mediated cell lysis.

Escherichia coli K-12 contains nine cryptic prophages that individually are incapable of producing active phage particles and constitute 3.6% of its genome (Wang et al., 2010). Rather than genomic junk, we found these cryptic prophages help the cell cope with stress (Wang et al., 2010). We also found that prophage genes are induced in *E. coli* during biofilm formation (Domka et al., 2007) and that cryptic prophage influence biofilm formation in this strain (García Contreras et al., 2008; Wang et al., 2010, 2009). Furthermore, active, filamentous phage influence the biofilm dispersal and phenotypic variation of *Pseudomonas aeruginosa* (Webb et al., 2004). Hence, cryptic and active phages are involved intimately in cell physiology in roles distinct from phage propagation.

Here, we became intrigued when we encountered a demarcation line between different swimming *E. coli* cells (Figure 1) and investigated the underlying mechanism. We screened the swimming behavior of 4,296 single-gene knockouts of the Keio collection (Baba et al., 2006) and found that the demarcation line disappears for a mutation related to phage development. By hypothesizing the gap between swimming cells was related to phage lysis, we identified a T1-type lytic phage (named SW1) that allows *E. coli* K-12 to recognize their own clonemates (this phage appears to arise from the Keio collection). By utilizing our strains devoid of each of the nine resident cryptic prophage in *E. coli* (Wang et al., 2010), we determined that the demarcation line is enhanced by putative methylase YfdM of cryptic phage CPS-53, and the extent of the demarcation line is directly related to the concentration of phage. Similar results were found with lysogenic phage lambda and ϕ80. Furthermore, we found commensal *E. coli* K-12 distinguishes itself from the pathogen enterohemorrhagic *E. coli* (EHEC); this recognition has not been identified previously as it was reported that *E. coli* K-12 is not sensitive to the phage of EHEC (Hernandez-Doria and

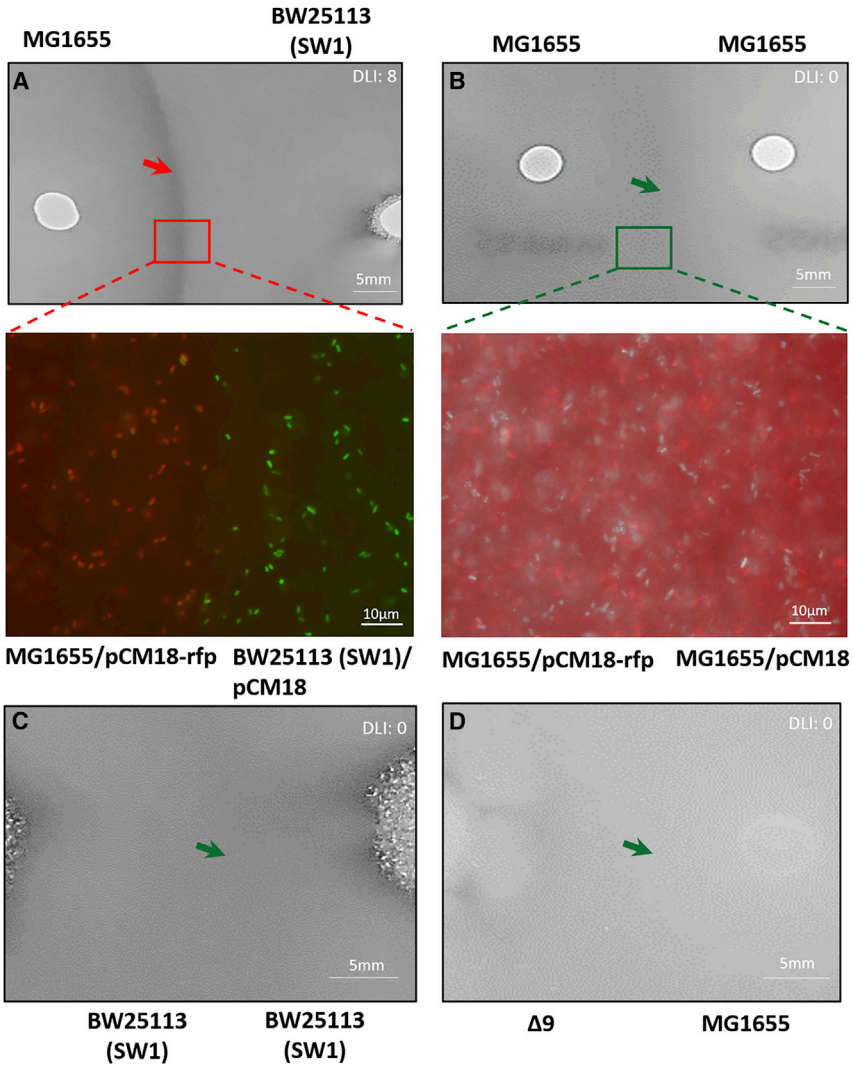

Figure 1. Demarcation Lines Develop between Siblings with Different Phage Content for Swimming Cells

(A) Upper panel: motility halos for MG1655 versus BW25113 (SW1); lower panel: non-mixing for siblings with different phage content (MG1655/pCM18-rfp appearing as red cells versus BW25113 (SW1)/pCM18 appearing as green cells).

(B) Upper panel: motility halos for MG1655 versus MG1655; lower panel: mixing for siblings that lack phage (MG1655/pCM18-rfp appearing as red cells versus MG1655/pCM18 appearing as green cells).

(C) Merging of two swimming motility halos for siblings with the same phage SW1, BW25113 (SW1) versus BW25113 (SW1).

(D) BW25113 (SW1) made unrecognizable by deleting all the cryptic prophage (BW15113 (SW1) Δ9, "Δ9") versus MG1655. Each plate contains two strains, and the green arrow indicates where the two swimming halos merge (demarcation line index (DLI) ≤ 3, indicated at upper right in photos) while the red arrow indicates the demarcation line (DLI ≥ 4). Scale bars indicate 5 mm for agar plates and 10 μm for microscopy images.

Sperandio, 2018). Hence, cells employ both active (lytic and temperate) phages and inactive phages (cryptic prophage CPS-53) to control cell to cell contact of commensal gastrointestinal tract bacteria. Although it is generally understood that phage lyse related bacteria that lack the corresponding phage, we argue here that lytic phage SW1 is not a mere contaminant but instead that the *E. coli* K-12 strain uses the phage to its benefit in a social sense; i.e., during nutrient foraging and immunity from other phages.

RESULTS

Phages Cause Bacteria to Form Demarcation Lines during Swimming Motility

We initially noticed a clear demarcation line between two different *E. coli* K-12 strains, MG1655 and BW25113, which is found later in this work to harbor lytic phage SW1 (henceforth BW25113 [SW1]) when inoculated on the same motility plate (Figure 1A); the demarcation line was absent for identical clones: BW25113 (SW1) versus BW25113 (SW1) and MG1655 versus MG1655 (Figures 1B and 1C). Hence, the demarcation line was only developed between non-identical strains.

To confirm the motility of identical cells was unaffected when their swimming halos meet, we labeled siblings (e.g., MG1655 versus MG1655) with either red fluorescent protein (RFP) and GFP and found complete mixing of individual cells in the demarcation line (Figure 1B). In contrast, for non-identical strains (i.e., MG1655 versus BW25113 [SW1]), we found that when their motility halos meet, there was no mixing of cells and a clear gap formed (Figure 1A).

The Demarcation Line between Siblings Depends on Cryptic Prophage CPS-53

We hypothesized the demarcation line was due to a secreted cell product; hence, we searched the complete *E. coli* K-12 library of single-gene knockouts (Keio collection based on BW25113) as a pooled library by plating approximately 10 colonies per motility plate, challenging with MG1655, and looking for the absence of the demarcation line as an indicator of a missing secreted protein. To better characterize the intersection of the two competing motility halos, we developed a demarcation line index (based on darkness, gap width, and consistency) with a value of 0 indicating complete merging and 10 indicating a completely formed demarcation line. This screen identified eight mutants (*yahO, yghG, rpoC, yecA, yfdC, ygeA, mhpA*, and *rep*) that had diminished demarcation lines (Figure S1). Of these, only the *rep* mutation completely eliminated the demarcation line. The *rep*

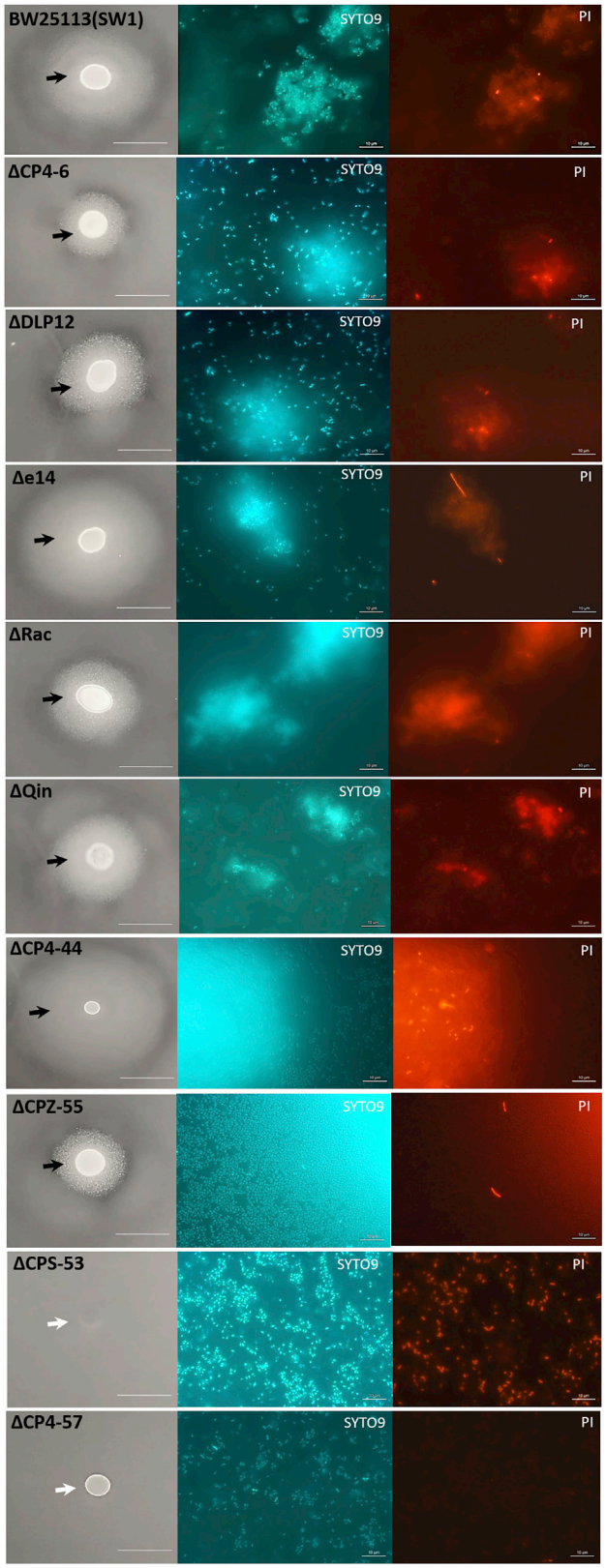

Figure 2. BW25113 Cryptic Prophage CPS-53 Is Required to Form a Colony Lysis Zone

Colony lysis zones for BW25113 (SW1) and the BW25113 single cryptic prophage deletion strains ΔCP4-6, ΔDLP12, Δe14, ΔRac, ΔQin, ΔCP4-44, ΔCPZ-55, ΔCPS-53 and ΔCP4-57. Left: motility agar plates. Middle: Syto9 staining of the precipitates outside the colony (showing all cells). Right: propidium iodide staining of the precipitates outside the colony (showing dead cells). Black arrows indicate cell lysis at the edge of the colony (indicating the presence of SW1 phage), and white arrows indicate the lack of cell lysis (indicating no phage). Scale bars indicate 10 mm for agar plates and 10 μm for microscopy images (middle and right). Representative images are shown.

mutation has been linked previously to a swimming and swarming defect (Girgis et al., 2007), and Rep is required for replication of some lysogenic bacteriophages, such as P2 (Calendar et al., 1970) as an ATP-dependent helicase. Therefore, we focused on phage-related proteins as necessary for the cell to make the demarcation line.

To efficiently check for relationship between the resident *E. coli* cryptic phage and the demarcation line, we tested the BW25113 (SW1) Δ9 strain that lacks all nine of the cryptic prophage (Wang et al., 2010) versus MG1655, and we found the two motility halos merged and the demarcation line was eliminated (Figure 1D); hence, phage-related proteins are responsible for the demarcation line and self-recognition.

We then tested each of the nine derivatives of BW25113 (SW1) with a single, complete cryptic prophage deletion (ΔCP4-6, ΔDLP12, Δe14, Δrac, ΔQin, ΔCP4-44, ΔCPS-53, ΔCPZ-55, and ΔCP4-57) (Wang et al., 2010) by spotting each strain by itself on motility plates and checking for a clearance zone at the colony periphery; therefore, this clearance zone is distinct from the demarcation line that forms when two motility halos meet. This colony lysis zone assay allowed us to examine the impacts of phage on the colony (a type of biofilm), on the cells just outside of the colony (including the viability of individual cells), and on the motility halo. We found that strains lacking cryptic prophages CPS-53 and CP4-57 failed to make a clearance zone beyond their colonies on a motility plate (Figure 2) and that deleting CPS-53 prevented BW25113 (SW1) from forming a clearance zone at the boundary of its colony (Figure 2). In comparison, some clearance at the colony boundary was seen for the strain that lacked CP4-57 (Figure 2). Hence, proteins related to cryptic prophage CPS-53 are required for the colony clearance zone and for the demarcation line. Note that the strain lacking CPS-53 is still susceptible to killing by SW1 (Figure S2A).

To test whether the complete CPS-53 phage or one its proteins is required to make the demarcation line, we tested 13 single gene mutants of CPS-53 and found that strains with a deletion in CPS-53 prophage genes *yfdQ* and *yfdM* eliminated the demarcation line with MG1655 (Figure S1C); *yfdQ* encodes an uncharacterized protein, and *yfdM* encodes a putative methylase. We then tested these mutants further by trying to restore the demarcation line in these CPS-53 mutants via production of each protein via pCA24N plasmids in its respective BW25113 (SW1) knockout strain and found production of YfdM in the *yfdM* host and YfdQ in the *yfdQ* host re-established the demarcation line with MG1655 (Figures S1D and S1E). Critically, production of these two CPS-53 proteins

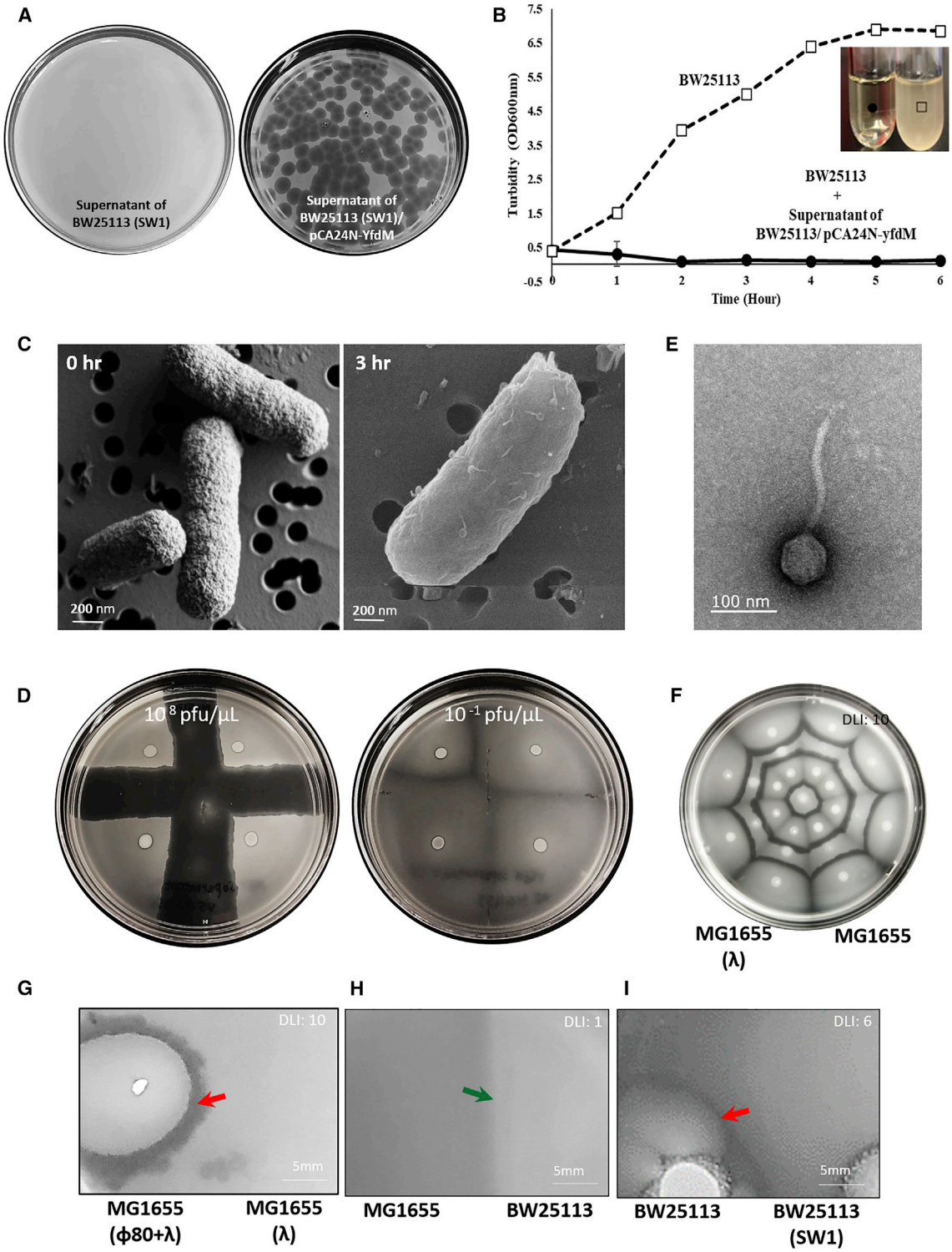

Figure 3. Production of CPS-53 Protein YfdM Creates Active Phages and a Demarcation Line from the Intersection of Two Swimming Motility Halos for Siblings with Different Phage Content

(A) Plaque assay with BW15113 (SW1) cells in soft agar for the filtered supernatant of BW15113 (SW1) and the filtered supernatant of BW25113 (SW1)/pCA24N-yfdM (right) showing plaques are only produced when YfdM is overproduced.

(B) Production of YfdM in BW25113 (SW1)/pCA24N-yfdM forms supernatants that lyse BW25113 (1% supernatant was added at time 0 and pictures of cultures are shown as insets with cell debris seen clearly from lysed cells).

(legend continued on next page)

generated hundreds of plaques with BW25113 (SW1) in the soft agar (Figure 3A for YfdM). In addition, as negative controls, production of either YfdM or YfdQ in the ΔCPS-53 strain did not produce plaques, production of YdfM in the absence of CPS-53 (i.e., ΔCPS-53/pCA24N-yfdM) did not cause a demarcation line to form with MG1655 (Figure S3A for YfdM), and production of YfdM in a CPS-53$^+$ strain that lacks SW1 did not produce plaques (i.e., BW25113 [no SW1]/pCA24N-yfdM, Figure S3B). These results show the demarcation line depends on cryptic prophage CPS-53 and its proteins YfdQ and YfdM. For the remaining experiments, we focused on YfdM since YfdQ is uncharacterized, and methylases are important for phage propagation (Roberts et al., 2004).

Lytic Phage SW1 Creates the Demarcation Line

Since we found plaques when YfdM was produced and since CPS-53 is a cryptic prophage unable to produce phage particles (Rudd, 1999), we hypothesized that the demarcation line is from cell lysis caused by a phage carried by the strain. To test for the presence of the phage, we produced YfdM from pCA24N-yfdM in BW25113 (SW1), added the supernatant to BW25113 (SW1) cells, and found a dramatic reduction in the turbidity of the cultures (Figure 3B). We then used scanning electron microscopy to obtain images of the cells at 0 h and 3 h and found the turbidity reduction was likely caused by phage particles that are seen clearly adhered to BW25113 (SW1) cells (Figure 3C). Therefore, producing YfdM in BW25113 (SW1) causes phage to form and cells to lyse.

To investigate whether the phage was related to the demarcation line, we made a phage lysis zone by adding (20 μL) of various concentrations of supernatant of BW25113 (SW1)/pCA24N-yfdM containing phage to the motility plate. The supernatant containing phage (10^8 pfu/μL) formed a thicker barrier between motile cells in a streak test than supernatants with less phage (10^{-1} pfu/μL) (Figure 3D), suggesting that it was phage causing the demarcation line when swimming cells meet.

To clarify this result, we tested whether the demarcation line between BW25113 (SW1)/pCA24N versus BW25113 (SW1)/pCA24N-yfdM depends on production of YfdM and found larger demarcation lines with increasing concentrations of isopropyl β-D-1-thiogalactopyranoside (IPTG) to induce *yfdM* (Figure S3C). Critically, the demarcation line only formed on the side of the motility halo where the halos meet; i.e., SW1 phage is primarily made by the infected strain when it meets siblings that lack phage.

Furthermore, to show the demarcation line is produced by cell lysis from SW1 phage, we took samples from the demarcation line and motility halo and performed plaque assays. After diluting the phage 100-fold, we found substantial cell lysis and plaque formation from the agar sample from the demarcation line, but no plaques formed from the motility halo sample (Figure S3D). Together with the preceding section, these results indicate that cryptic prophage CPS-53 controls the production of active SW1 phage particles and that lysis by this lytic phage is responsible for producing the demarcation line. This defective-helper relationship has been seen previously in EHEC temperate phages (Asadulghani et al., 2009).

Characterizing Phage SW1

To characterize the phage associated with BW25113 (SW1), we captured transmission electron micrograph images of the phage made from the supernatants of BW25113 (SW1)/pCA24N-yfdM (Figure 3E). The phage formed round plaques 5 mm in diameter on a lawn of BW25113 (SW1) cells (Figure 3A); the phage capsid is approximately 71 nm in diameter, and the non-contractile tail is approximately 205 nm. Hence, it is a family Siphoviridae phage based on its morphology (Figure 3E). We suggest the name Escherichia phage vB_EcoS-SW1 (SW1 hereafter) based on the naming convention (Adriaenssens and Brister, 2017).

By sequencing the DNA of the phage particles, we determined SW1 is a phage (49,096 bp; Table S1; Figure S4; GenBank: PRJNA498536) that is similar to lytic phage T1 (85% identity, 48,836 bp; GenBank: AY216660) and phage vB_EcoS_SH2 (99% identity, 49,088 bp; GenBank: Y985004). PCR of the three SW1 phage genes (exonuclease, tail fiber, and recombinase) confirmed that SW1 is not present in the BW25113 (SW1) or MG1655 genome; hence, it is a lytic phage (so it does not exist in the genome as a lysogen but exists extracellularly) (Figures S5A and S5B). Corroborating this, both an integrase and excisionase usually associated with lysogeny are not present in the SW1 genome (Table S1). Further evidence that SW1 is similar to T1 was found by selecting strains from a pooled Keio collection that could grow in the presence of SW1 phage particles. After sequencing to identify the mutations that prevented SW1 lysis, we found that BW25113 (SW1) cells with a *fhuA* (14 times) or *tonB* (1 time) mutation are less sensitive to SW1. FhuA is the attachment protein for T1 (Böhm et al., 2001; Langenscheid et al., 2004), and we found the *fhuA* mutant is nearly completely resistant to SW1 with both a soft agar and a liquid culture assay (Figure S2). In addition, SW1 could not be detected in the *fhuA* mutant via PCR. TonB is necessary for T1 transfer through the membrane (Böhm et al., 2001; Langenscheid et al., 2004), and we found the *tonB* mutant is 10^7 times more resistant than the wild-type strain but not almost completely resistant like *fhuA* (Figure S2). Hence, SW1 is a T1-type, lytic phage.

(C) SEM image of the phage particles formed by producing YfdM in BW25113 (SW1)/pCA24N-yfdM that adhere and lyse BW25113 (SW1). Cells shown prior to phage addition (0 h) and after phage build-up (3 h). Scale bars indicate 200 nm.
(D) Phage lysis zone between MG1655 motility halos created by inoculating cells (5 μL) in four locations on a motility plate containing phage from filtered supernatant of BW25113 (SW1)/pCA24N-yfdM (which overproduces phage SW1) in 5 μL at two concentrations: 10^8 pfu/μL and 10^{-1} pfu/μL (right).
(E) TEM image of the phage particles formed by producing YfdM in BW25113/pCA24N-yfdM (amplified 20,000-fold). One representative image is shown. Scale bar indicates 100 nm.
(F–I) Motility halos for (F) alternating inoculations of MG1655 with phage lambda (center) and without phage lambda (next concentric circle with eight inoculations), (G) MG1655 with phages ϕ80 + lambda versus MG1655 with phage lambda, (H) MG1655 versus BW25113, and (I) BW25113 versus BW25113 (SW1). Each plate contains two strains, and the green arrow indicates where the two swimming halos merge (demarcation line index (DLI) $\leq$ 3, indicated at upper right in photos) while the red arrow indicates the demarcation line (DLI $\geq$ 4). Scale bars indicate 5 mm for agar plates.

Lysogenic Phages Lambda and ϕ80 Create a Demarcation Line

To ensure the plaques generated by producing YfdM in BW25113 (SW1) were solely related to CPS-53, we tested BW25113 (SW1) and found it did not contain lambda phage nor did it contain phage ϕ80 (Figures S5C and S5D). To corroborate the formation of the demarcation line is by lysis by SW1, we tested a MG1655 strain that harbors phage lambda. When MG1655 lacking lambda was placed on motility plates with MG1655 containing lambda, a clear demarcation line was formed (Figure 3F). In addition, MG1655 with lysogenic lambda phage formed a demarcation line with MG1655 with both lysogenic ϕ80 and lambda (Figure 3G). Hence, demarcation lines are formed from cell lysis due to phage when one of the strains lacks the phage. Furthermore two phages cause a more extensive demarcation line to form. We also found the lambda-resistant strain BW25113 *lamB* does not form a demarcation line with BW25113 infected with lambda (Data S1Aa); hence, there is preferential lysis of the non-infected strain when a demarcation line forms. These results indicate that phages are shed by the lysogens, and these phages are used to kill siblings that are not infected.

To corroborate this result, we tested whether BW25113 lacking SW1 phage (obtained from the Coli Genetic Stock Center) forms a demarcation line with MG1655 and found that without SW1, BW25113 does not form a demarcation line with MG1655 (Figure 3H). As expected, BW25113 forms a demarcation line with BW25113 infected with the SW1 phage (Figure 3I). In addition, BW25113 (SW1) forms a demarcation line with the lambda-resistant strain BW25113 *lamB;* hence, the demarcation line caused by phage SW1 is not related to lambda phage.

Colonies with Phages Form a Colony Lysis Zone on Motility Plates

Observation of spotted colonies on motility plates provided additional evidence of the presence of phage and cell lysis. By examining individual cells in the colony lysis zone, we found SW1 kills cells that carry it just outside the colony to form precipitates we termed crystals (Data S1Ab); the diffuse staining by Syto9 and propidium iodide indicates the presence of extracellular DNA from lysis. In contrast, cells carrying phage SW1 in the motility halo (in the absence of a demarcation line) are dense and show no sign of lysis (Data S1Ab). Furthermore, this single-strain analysis shows that only cells that lack cryptic prophages CPS-53 and CP4-57 fail to a produce colony lysis zone with crystals, although the ΔCP4-57 strain has a gap between the colony and its motility halo (Figure 2). Note there is cell death in the ΔCPS-53 sample (about 50% of the cells are dead and stain red with propidium iodide); however, this is not related to SW1 phage since this strain has high motility and the whole motility halo resembles a colony, which is a type of dense biofilm, and all of the prophage mutants and wild-type strain have a significant number of dead cells in their colonies.

We also found this colony lysis zone phenomenon for MG1655 including phages lambda and ϕ80, whereas the MG1655 lacking phage does not show this phenotype (Data S1Ba). In addition, MG1655 infected by SW1 phage also has a colony lysis zone (Data S1Ba). These results demonstrate that the presence of active phage can be discerned from the colony lysis zone for colonies on motility plates and that some of the infected cells lyse.

Moreover, by using the colony lysis zone approach, we found that colonies of BW25113 Δ*yfdM* and BW25113 ΔCPS-53 were not changed by SW1 phage infection (Data S1C). Hence, the absence of the colony lysis zone shows again the dependence of SW1 on proteins of cryptic prophage CPS-53, specifically, the dependence on YfdM.

Cells Lyse in the Demarcation Line Due to Phage

To determine the role of phage in self-recognition, we investigated whether cells lyse in the demarcation line when phage are produced. We found that although the demarcation line appears clear on motility plates, there are some cells in this zone, and their numbers are about 10-fold less than in the periphery of the swimming halo (Data S1D; Table S1). Critically, we found that for strains that produce a demarcation line, i.e., for MG1655 versus BW25113 (SW1) and for BW25113 (SW1)/pCA24N-yfdM versus BW25113 (SW1)/pCA24N, cells are dead in the demarcation line (Data S1D; Figure 4), which indicates phage propagation (i.e., lysis) throughout its swimming halo. In contrast, for strains not producing a demarcation line; i.e., for BW25113 (SW1)/pCA24N versus BW25113 (SW1)/pCA24N (Data S1E), all the cells were healthy and unlysed in the merging motility halos. Notably, SW1 primarily kills the strain not producing YfdM as the swimming halos meet (Figure 4) since motile cells producing YfdM near the demarcation line show little death, while cells of the other halo near the demarcation line are nearly all dead. These results demonstrate clearly that the demarcation line is formed from the lysis of siblings that lack SW1 and that siblings infected with SW1 have some immunity from cell lysis by phage SW1 when swimming cells meet. Note escape flares are frequently seen (Figure 4), but since the demarcation line formed by these flares is strong, these are probably due to differences in the number of cells that escape killing by phage SW1 in the colony lysis zone and make the motility halo (Figure 2) rather than the development SW1-resistant *fhuA* mutants.

YfdM and Phage SW1 Are Used to Distinguish Siblings

On the basis of our results, we reasoned that cells could be made to no longer recognize siblings if one strain over-produced phage. Verifying this hypothesis, overproduction of CPS-53 phage protein YfdM in BW25113 leading to overproduction of phage caused the formation of a very large demarcation line with BW25113 (SW1)/pCA24N (Figure 5A) in which cells were clearly killed. In contrast, without YfdM production, the two BW25113 (SW1) strains merged perfectly (Figure 5B). In addition, production of YfdM in the absence of CPS-53 in both strains was unable to produce a demarcation line (Figure 5C). Additionally, production of YfdM in MG1655 (i.e., MG1655/pCA24N-yfdM) was unable to produce a demarcation line with MG1655/pCA24N (Figure 5D), since MG1655 lacks phage SW1. As expected, two MG1655/pCA24N strains merge perfectly (Figure 5E). Therefore, YfdM together with SW1 are necessary to form the demarcation line in BW25113, and siblings can be distinguished by the production of phage.

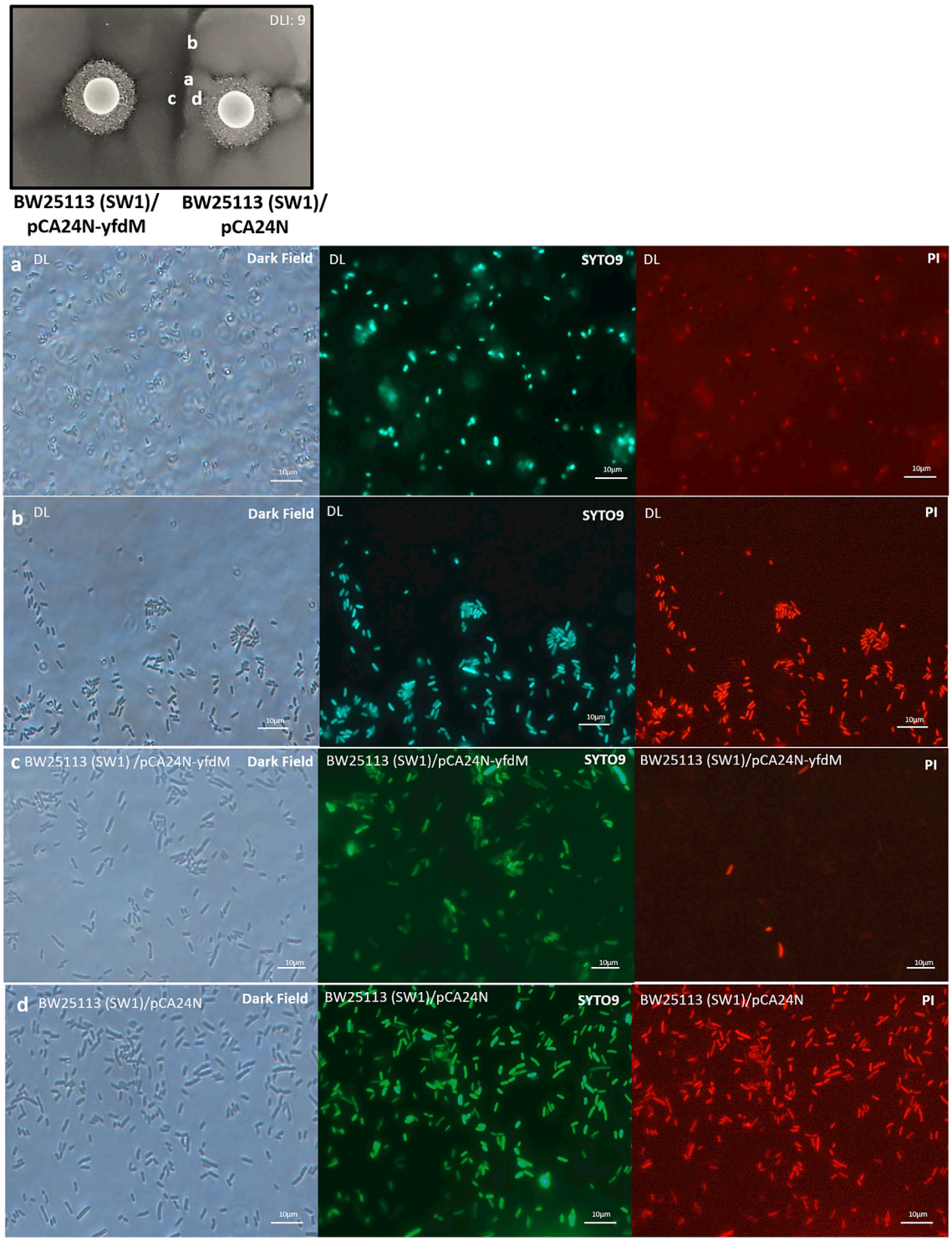

Figure 4. Cell Death Causes the Demarcation Line

Live/dead staining of the intersection of the swimming motility halos of BW15113 (SW1)/pCA24N-yfdM versus BW25113/pCA24N. Upper panel: photo letters "a," "b," "c," and "d" indicate the position imaged in the fluorescence microscope. Lower panel: left shows dark field, middle shows all cells stained by Syto9, and right shows dead cells stained by propidium iodide. Scale bars indicate 10 μm for microscopy images. Representative images are shown. Note the inconsistency in the Styo 9 stain color is due to optimizing image resolution.

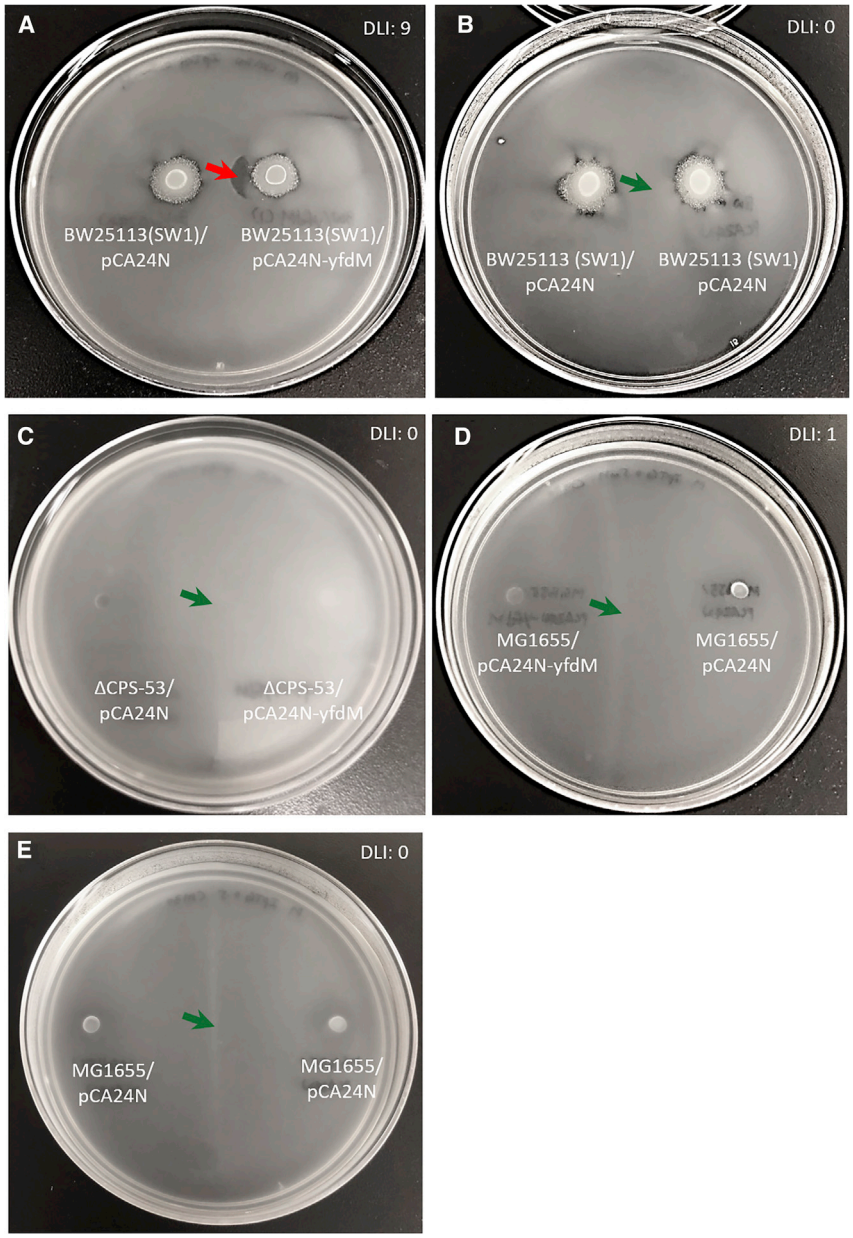

Figure 5. Production of CPS-53 Protein YfdM Creates a Sharp Demarcation Line in the Presence of SW1

Intersection of swimming motility halos of (A) BW25113 (SW1)/pCA24N versus BW25113 (SW1)/pCA24N-yfdM, (B) BW15113 (SW1)/pCA24N versus BW15113 (SW1)/pCA24N, (C) ΔCPS-53/pCA24N versus ΔCPS-53/pCA24N-yfdM, (D) MG1655/pCA24N-yfdM versus MG1655/pCA24N, and (E) MG1655/pCA24N versus MG1655/pCA24N. YfdM was produced from pCA24N-yfdM with 0.5 mM IPTG. Each plate contains two strains, and the green arrow indicates where the two swimming halos merge (demarcation line index (DLI) $\leq$ 3, indicated at upper right in photos) while the red arrow indicates the demarcation line (DLI $\geq$ 4). Representative images are shown. Note the lines seen for (C) and (D) are due to the accumulation of cells at the place where the motility halos combine.

To confirm that siblings can be distinguished through phage, we infected MG1655 with SW1 phage and tested whether a demarcation line could be created with MG1655 that lack phage SW1. We found MG1655 with phage SW1 forms a large demarcation line with MG1655 that lacks SW1; hence, again, phage can be used to distinguish siblings (Data S1Bb). Similarly, we infected the non-laboratory strains *E. coli* K-12 ATCC 25404 and ATCC11303 with SW1 and found a demarcation line forms only in the infected strain versus MG1655 (Data S1F).

SW1 Allows Cells to Recognize EHEC

Additionally, we investigated whether commensal K-12 could recognize pathogenic bacteria, such as EHEC, through the use of phage. We found K-12 with SW1 formed a demarcation line with EHEC (Data S1G); in contrast, the swimming halos of two EHEC colonies merged. These results confirm siblings can distinguish clonemates (and not form a demarcation line) and that lysis occurs when two different strains meet and have different phages. In addition, EHEC colonies have a colony lysis zone (Data S1Gj), and EHEC swimming cells form a smaller but discernable demarcation line with the K-12 strain that lacks SW1 (Data S1Gc and S1Gd), indicating EHEC also uses its own active phage particles (Asadulghani et al., 2009) for self-recognition. Further proof that EHEC phage recognizes *E. coli* K-12 is that we found that phage particles isolated from EHEC form plaques with both BW25113 (SW1) and BW25113 that lacks SW1 (Data S1Gk and S1Gl). We identified the EHEC phage that is active on K-12 as 933W (Data S1H). To confirm that EHEC competes with *E. coli* K-12 and that there is a conditional fitness advantage to being infected with SW1, we tested the resistance of BW25113 (SW1) versus EHEC with purified SW1 phage and with EHEC phage. Phage was added to flasks containing both strains, and the surviving cells were counted based on their color difference. The results show that BW25113 (SW1) is only slightly more resistant to both SW1 and EHEC phage compared with EHEC (Figure 6A); this result is expected since both bacteria already have phage and therefore some immunity when challenged with different phages. Overall, EHEC competes with *E. coli* K-12 and forms a demarcation line, but the presence of phage SW1 in K-12 and numerous phages in EHEC provide some immunity to each strain.

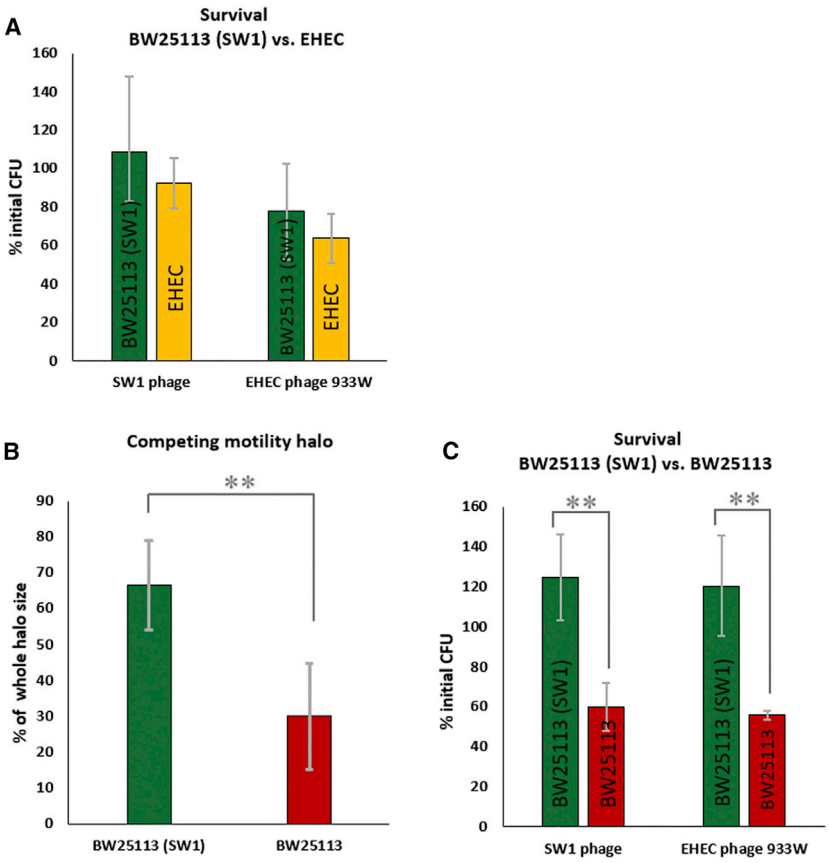

Figure 6. SW1 Increases the Competitiveness of BW25113

(A) Survival of BW25113 (SW1)/pCM18 versus EHEC/pCM18-rfp after adding purified of SW1 (10^8 PFU/mL) or EHEC phage 933W (10^2 PFU/mL). Equal numbers of cells were mixed, phage was added for 1 h, then surviving cells were plated and identified based on their colony color. The data show the percentage of the initial cell number (CFU) from four independent cultures.

(B) Average of competing motility halo sizes for BW25113 (SW1)/pCM18 versus BW25113/pCM18-rfp on the same motility agar plate. Each motility plate contains two strains, and the halo sizes were measured by ImageJ. The data show the percentage of the combined halo area for both stains as analyzed from six independent cultures. A representative motility plate is shown in Data S1I. **$p < 0.01$ indicates significant differences between BW25113 and BW25113 (SW1) via a one-way ANOVA.

(C) Survival of BW25113 (SW1)/pCM18 versus BW25113/pCM18-rfp after adding purified SW1 (10^8 PFU/mL) or EHEC phage 933W (10^2 PFU/mL). **$p < 0.01$ indicates significant differences between BW25113 and BW25113 (SW1) via a one-way ANOVA (four independent cultures).

SW1 Increases Cell Fitness with Siblings Conditionally

To determine whether SW1 increases cell fitness for siblings that that contain SW1, we labeled cells to distinguish their motility halos and monitored swimming motility for BW25113 (SW1) versus BW25113. In six out of seven trials, cells infected with SW1 engulfed those that lack SW1 showing the lytic phage SW1 provides a demonstrable benefit during nutrient foraging (Figure 6B; Data S1Ia). Independently, the motility of the two strains was not significantly different (Data S1Ib and S1Ic). To confirm the increase in fitness with SW1, we tested the growth of BW25113 (SW1) relative to BW25113 when challenged with purified SW1 phage or when challenged with purified EHEC phage. Phage were added to flasks containing both strains, and surviving cells were counted based on the colony color cells. Critically, the results show that BW25113 (SW1) is far more resistant to both SW1 phage and EHEC phage compared with BW25113 (Figure 6C). Hence, the presence of lytic phage SW1 confers a competitive advantage when challenged with SW1 and phage from other strains.

Origin of Phage SW1

To determine the source of the SW1 phage, we used the colony lysis zone assay for nine random Keio mutants since we originally found the colony lysis zone in our BW25113 wild-type stock from the Keio collection (Baba et al., 2006). We found the colony lysis zone in five Keio mutants from the original source plates (Data S1Ja), and three of these strains, 15-G9, 15-E6, and 63-D7, had phage when YfdM was produced (1 to 6 pfu/100 μL). In contrast, the Keio strains that do not have a colony lysis zone, such as 55-3D, did not have phage with YfdM production (Data S1Jb). Also, we checked hundreds of Keio mutants for the Dienes line assay with MG1655, and most of the mutants formed a demarcation line indicating the presence of SW1 (Figure S1). Hence, phage SW1 may be pervasive through dissemination of the Keio collection (and visible in specific clones via the colony lysis zone assay). Since SW1 is a T1-type phage, and T1 is notoriously difficult to remove, we feel SW1 is also robust like T1 and readily propagates when cells contain cryptic prophage CPS-53.

Full activation of SW1 (i.e., plaques formed) requires production of YfdQ or putative Dam methylase YfdM of cryptic prophage CPS-53 (e.g., pCA24N-yfdM). Since neither protein has been characterized and it is unlikely others would have cause to check for plaque formation with these specific supernatants, SW1 was not detected previously. Formation of the demarcation line to detect SW1 would require studying motility with two different Keio clones for the case where only one of them was infected with SW1, since if both clones were infected or if neither clone were infected, their halos would merge. Of course, a demarcation line would be seen if an infected Keio clone (or wild-type) were studied in a motility experiment with an uninfected but susceptible strain (e.g., MG1655), as we fortuitously did in this work.

DISCUSSION

We demonstrate here that cells use phage for self-recognition. Hence, during motility, when two strains meet and one strain

lacks a phage to which it is sensitive, a clearance zone forms in which the cells that lack the phage are lysed (Figure 4; Data S1D). Although we did not investigate the role of phage in biofilms (we focused on swimming motility, a planktonic phenotype), we anticipate that similar principles apply and that phage-containing cells have a conditional fitness advantage over non-phage-containing cells.

We also demonstrate here that commensal *E. coli* uses cell killing based on proteins from cryptic prophage CPS-53 (e.g., YfdM, YfdQ) to activate lytic phage SW1 to differentiate itself from siblings that lack phage. Hence, our results show a surprising dependence of lytic phage SW1 on cryptic prophage proteins; this result provides insight into the conditional benefit of cells harboring cryptic prophage. Of course, dependence on chromosomal proteins (i.e., non-cryptic prophage proteins) has been demonstrated previously with T1-type phage; for example, as we found here, FhuA is required for attachment, and TonB is required for transfer phage through the cell membrane (Böhm et al., 2001; Langenscheid et al., 2004). Critically, YfdM of CPS-53 has 91 aa in common with the Dam methylase of EHEC Stx2 phage (Ogura et al., 2015), and T1 requires Dam. Moreover, putative methylase YfdM is not related to the Dam methylase of SW1 or BW25113, so it should provide a novel methylase function. Hence, SW1 appears to use the putative Dam methylase of CPS-53 (i.e., YfdM) to make active phage. Supporting this hypothesis, bacteriophage P1 cleaves its DNA at a packing site (*pac*) once it is methylated by adenine methylase (Fujisawa and Morita, 1997; Sternberg and Coulby, 1990), and T1 also has a *pac* site (Roberts et al., 2004). Hence, YfdM of CPS-53 might methylate a *pac*-like site of SW1 to signal DNA cleavage for filling the prohead with DNA during phage packaging, and this methylase activity may limit DNA packaging (Roberts et al., 2004). Evidence of this is that we only see large numbers of plaques in the presence of overproduced YfdM (Figure 3A). However, SW1 propagates whenever there is a wild-type copy of $yfdM^+$ in the chromosome (but not to the extent that plaques are readily formed). Alternatively, putative methylase YfdM may facilitate SW1 proliferation by protecting it from restriction enzyme attack.

Since some cell death occurs in the absence of neighboring cells (see the colony lysis zones around colonies on motility plates [Figure 2; Data S1Ab]), the use of lytic phage imposes some cost. Overall, the use of lytic phage particles should increase the conditional fitness of commensal *E. coli* as long as there is more lysis of the competing cells. Critically, SW1 becomes active primarily where the motility halos of siblings infected with phage and siblings lacking phage meet (and not in other parts of the halo of the SW1-infected cells) since a large, one-sided demarcation line (“crescent moon” shape) is clearly visible when SW1 concentrations are large (due to production of YfdM) (Figure 5A; Data S1Bb). What remains to be determined is how siblings are protected from phage SW1 since clearly two siblings infected with phage have no demarcation line (Figure 1C) and no lysis when their halos meet (Data S1E). Perhaps, lysis from SW1 is growth-phase dependent (giving rise to the colony lysis zones of Figure 2 and Data S1Ab) or there is a SW1 protein that delays lysis and gives immunity as SW1 exists as a pseudolysogen (phage carrier cell) (Cenens et al., 2013) in which SW1 is replicating autonomously and at a low frequency releases phage. When a swimming halo is met of siblings that are not infected, perhaps a signal causes more phage to be released, resulting in lysis primarily of the noninfected strain. Since for lysogenic phage, such as lambda and ϕ80, there should be phage immunity for the phage-bearing strain (Ptashne et al., 1976; Thieffry and Thomas, 1995), it could be argued that the phage-containing strain should have an even greater fitness advantage over the phage-minus strain; however, we found evidence of lysis in the absence of competing strains for lysogens as well (Data S1Ba).

The primary benefit for cells infected with SW1 is the fitness advantage relative to cells that lack SW1 when the cells forage for food or when challenged by other phage, like that of EHEC, since we show cells infected with SW1 are more competitive under these two conditions (Figure 6B-6C). Furthermore, the benefit of retaining cryptic prophage is that without CPS-53, the cells are still susceptible to SW1 infection (Figure S2), and the cells do not have any of the benefits since they cannot produce enough SW1 to lyse significant numbers of siblings that lack SW1 (Figure 5C). Hence, there is an advantage to being infected with SW1 (a lytic phage) and an advantage to making more phage progeny by having CPS-53 (Figure 7).

In the gastrointestinal tract, commensal *E. coli* cells must compete with around 1,000 other bacterial species, whose combined density reaches 10^{12} organisms per gram (Wall, 2016). In addition, about five different *E. coli* strains usually colonize each human gastrointestinal tract (Conway and Cohen, 2015), and the chief competitor of pathogenic *E. coli* (Huynh et al.) in the gastrointestinal tract is *E. coli* K-12 (Bäumler and Sperandio, 2016). We demonstrated that a demarcation line is formed between these two strains that requires the phages of both EHEC and BW25113 (SW1), since EHEC forms a demarcation line with BW25113 that lacks phage, but the demarcation line is less strong when there is only phage from EHEC (Data S1Gc and S1Gd). We also found phages from EHEC form plaques on BW25113 (Data S1Gk and S1Gl) by utilizing the 933W phage. Furthermore, we found that the presence of SW1 makes BW25113 more competitive during nutrient foraging (Figure 6B). Hence, self-recognition may be important for the success of this commensal bacterium in increasing its fitness in colonizing humans, since it is a non-dominant strain (Gorbach, 1996), and it must compete with similar *E. coli* strains. Determining the role of this phage-mediated self-recognition *in vivo* should be explored.

Note that there are many phages in the gastrointestinal tract (Breitbart et al., 2003), and the slow growth of *E. coli* in this environment has led to pseudolysogeny of the virulent phage T4 (Los et al., 2003); hence, the use of phage for self-recognition is reasonable. This approach for self-recognition is also general, based on our results with three phages including both lytic (e.g., SW1) and lysogenic phage (e.g., lambda, ϕ80), and based on our results with three commensal *E. coli* (BW25113, ATCC25404, and ATCC11303) and pathogenic *E. coli* (Huynh et al., 2012). For these results, no overproduction of proteins like putative methylase YfdM is required to see a clear demarcation line when motility halos meet.

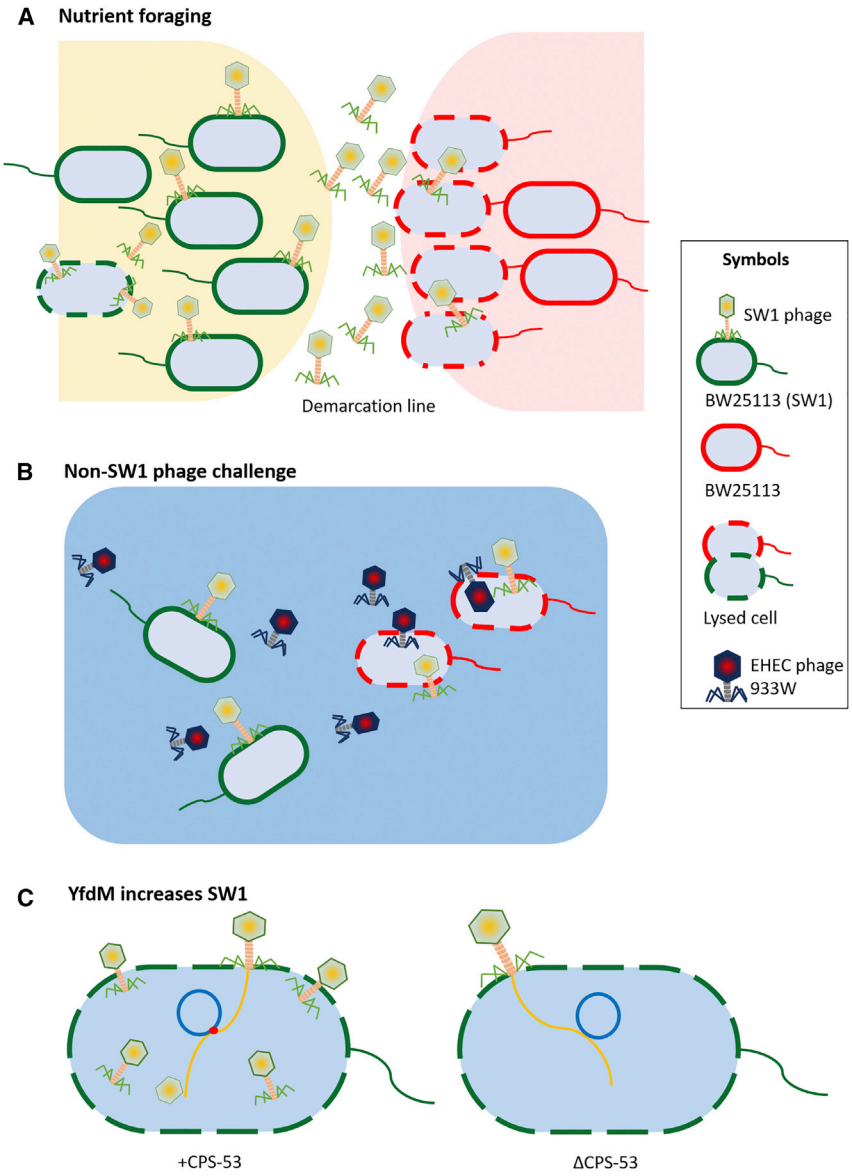

Figure 7. Schematic Illustration of the Conditional Benefits from SW1 Infection of *E. coli* K-12

Benefits are shown for nutrient foraging where siblings lacking SW1 are preferentially lysed (A), for non-SW1 phage challenge (e.g., EHEC phage) where siblings lacking SW1 are preferentially lysed (B), and for the presence of cryptic prophage CPS-53 where YfdM increases the titer of SW1 (cells that lack CPS-53 are susceptible to SW1 but make less SW1) (C).

Overall, our results suggest a bacterial cell infected by a lytic phage may have conditional benefits over siblings that lack the phage; for example, while obtaining scarce resources or when encountering other phages. In addition, these benefits rely on the infected strain utilizing the tools it obtained from an old enemy, a cryptic prophage (Figure 7).

STAR★METHODS

Detailed methods are provided in the online version of this paper and include the following:

- KEY RESOURCES TABLE
- CONTACT FOR REAGENT AND RESOURCE SHARING
- EXPERIMENTAL MODEL AND SUBJECT DETAILS
- METHOD DETAILS
  - Motility halo assay
  - Screening via the pooled Keio collection
  - Gel pad microscopy with GFP/RFP-labeled strains
  - Plaque assay
  - Polymerase chain reaction (PCR) to detect phages
  - Electron microscopy
  - Viability assay
  - Infection with SW1 phage
  - Infection with lambda phage
  - Phage DNA genome sequencing
- QUANTIFICATION AND STATISTICAL ANALYSIS
  - Scoring via the demarcation line index (DLI)
  - Statistical analysis
- DATA AND SOFTWARE AVAILABILITY

SUPPLEMENTAL INFORMATION

Supplemental Information can be found online at https://doi.org/10.1016/j.celrep.2019.03.070.

ACKNOWLEDGMENTS

We are grateful for the pooled Keio library provided by Dr. Justin Gallivan and for the TEM and SEM images provided by Missy Hazen of the Huck Institutes of the Life Sciences at the Pennsylvania State University. This work was supported by the Army Research Office (W911NF-14-1-0279 to T.K.W.), funds derived from the Biotechnology Endowed Professorship at the Pennsylvania State University (to T.K.W.), the National Key R&D Program of China (2018YFC1406500 to X.W.), the National Natural Science Foundation of China (31625001 to X.W.), and the KRIBB Initiative Research Program (to J.S.K.).

AUTHOR CONTRIBUTIONS

S.Y.S., Y.G., and J.S.K. conducted the experiments. X.W. and T.K.W. conceived the project. S.Y.S. and T.K.W. wrote the manuscript.

DECLARATION OF INTERESTS

The authors declare no competing interests.

Received: November 21, 2018
Revised: February 7, 2019
Accepted: March 18, 2019
Published: April 16, 2019

REFERENCES

Adriaenssens, E., and Brister, J.R. (2017). How to Name and Classify Your Phage: An Informal Guide. Viruses *9*, 70.

Alberti, L., and Harshey, R.M. (1990). Differentiation of *Serratia marcescens* 274 into swimmer and swarmer cells. J. Bacteriol. *172*, 4322–4328.

Armitage, J.P. (1992). Bacterial motility and chemotaxis. Sci. Prog. *76*, 451–477.

Asadulghani, M., Ogura, Y., Ooka, T., Itoh, T., Sawaguchi, A., Iguchi, A., Nakayama, K., and Hayashi, T. (2009). The defective prophage pool of *Escherichia coli* O157: prophage-prophage interactions potentiate horizontal transfer of virulence determinants. PLoS Pathog. *5*, e1000408.

Baba, T., Ara, T., Hasegawa, M., Takai, Y., Okumura, Y., Baba, M., Datsenko, K.A., Tomita, M., Wanner, B.L., and Mori, H. (2006). Construction of *Escherichia coli* K-12 in-frame, single-gene knockout mutants: the Keio collection. Mol Syst Biol. *2*, 2006.0008.

Bäumler, A.J., and Sperandio, V. (2016). Interactions between the microbiota and pathogenic bacteria in the gut. Nature *535*, 85–93.

Böhm, J., Lambert, O., Frangakis, A.S., Letellier, L., Baumeister, W., and Rigaud, J.L. (2001). FhuA-mediated phage genome transfer into liposomes: a cryo-electron tomography study. Curr. Biol. *11*, 1168–1175.

Breitbart, M., Hewson, I., Felts, B., Mahaffy, J.M., Nulton, J., Salamon, P., and Rohwer, F. (2003). Metagenomic analyses of an uncultured viral community from human feces. J. Bacteriol. *185*, 6220–6223.

Calendar, R., Lindqvist, B., Sironi, G., and Clark, A.J. (1970). Characterization of REP- mutants and their interaction with P2 phage. Virology *40*, 72–83.

Cardarelli, L., Saak, C., and Gibbs, K.A. (2015). Two Proteins Form a Heteromeric Bacterial Self-Recognition Complex in Which Variable Subdomains Determine Allele-Restricted Binding. MBio *6*, e00251–e00215.

Cenens, W., Makumi, A., Mebrhatu, M.T., Lavigne, R., and Aertsen, A. (2013). Phage-host interactions during pseudolysogeny: Lessons from the Pid/dgo interaction. Bacteriophage *3*, e1003269.

Conway, T., and Cohen, P.S. (2015). Commensal and Pathogenic *Escherichia coli* Metabolism in the Gut. Microbiol. Spectr. *3*, MBP-0006–MBP-2014.

Cooper, H.S., Murthy, S.N.S., Shah, R.S., and Sedergran, D.J. (1993). Clinicopathologic study of dextran sulfate sodium experimental murine colitis. Lab. Invest. *69*, 238–249.

Dey, A., Vassallo, C.N., Conklin, A.C., Pathak, D.T., Troselj, V., and Wall, D. (2016). Sibling Rivalry in *Myxococcus xanthus* Is Mediated by Kin Recognition and a Polyploid Prophage. J. Bacteriol. *198*, 994–1004.

Domka, J., Lee, J., Bansal, T., and Wood, T.K. (2007). Temporal gene-expression in *Escherichia coli* K-12 biofilms. Environ. Microbiol. *9*, 332–346.

Eisenstark, A. (1967). Bacteriophage Techniques. J. Virol. Methods *1*, 449–524.

Fujisawa, H., and Morita, M. (1997). Phage DNA packaging. Genes Cells *2*, 537–545.

García-Contreras, R., Zhang, X.-S., Kim, Y., and Wood, T.K. (2008). Protein translation and cell death: the role of rare tRNAs in biofilm formation and in activating dormant phage killer genes. PLoS ONE *3*, e2394.

Gibbs, K.A., Urbanowski, M.L., and Greenberg, E.P. (2008). Genetic determinants of self identity and social recognition in bacteria. Science *321*, 256–259.

Girgis, H.S., Liu, Y., Ryu, W.S., and Tavazoie, S. (2007). A comprehensive genetic characterization of bacterial motility. PLoS Genet. *3*, e154.

Gorbach, S.L. (1996). Microbiology of the Gastrointestinal Tract. In Medical Microbiology, S. Baron, ed. (University of Texas Medical Branch at Galveston).

Hansen, M.C., Palmer, R.J., Jr., Udsen, C., White, D.C., and Molin, S. (2001). Assessment of GFP fluorescence in cells of *Streptococcus gordonii* under conditions of low pH and low oxygen concentration. Microbiology *147*, 1383–1391.

Harrison, J.J., Wade, W.D., Akierman, S., Vacchi-Suzzi, C., Stremick, C.A., Turner, R.J., and Ceri, H. (2009). The chromosomal toxin gene *yafQ* is a determinant of multidrug tolerance for *Escherichia coli* growing in a biofilm. Antimicrob. Agents Chemother. *53*, 2253–2258.

Hernandez-Doria, J.D., and Sperandio, V. (2018). Bacteriophage Transcription Factor Cro Regulates Virulence Gene Expression in Enterohemorrhagic *Escherichia coli*. Cell Host Microbe *23*, 607–617.e6.

Hong, S.H., Hegde, M., Kim, J., Wang, X., Jayaraman, A., and Wood, T.K. (2012). Synthetic quorum-sensing circuit to control consortial biofilm formation and dispersal in a microfluidic device. Nat. Commun. *3*, 613.

Huynh, T.T., McDougald, D., Klebensberger, J., Al Qarni, B., Barraud, N., Rice, S.A., Kjelleberg, S., and Schleheck, D. (2012). Glucose starvation-induced dispersal of *Pseudomonas aeruginosa* biofilms is cAMP and energy dependent. PLoS ONE *7*, e42874.

Kitagawa, M., Ara, T., Arifuzzaman, M., Ioka-Nakamichi, T., Inamoto, E., Toyonaga, H., and Mori, H. (2005). Complete set of ORF clones of *Escherichia coli* ASKA library (a complete set of E. coli K-12 ORF archive): unique resources for biological research. DNA Res. *12*, 291–299.

Kusek, J.W., and Herman, L.G. (1980). Typing of *Proteus mirabilis* by bacteriocin production and sensitivity as a possible epidemiological marker. J. Clin. Microbiol. *12*, 112–120.

Langenscheid, J., Killmann, H., and Braun, V. (2004). A FhuA mutant of Escherichia coli is infected by phage T1-independent of TonB. FEMS Microbiol. Lett. *234*, 133–137.

Los, M., Wegrzyn, G., and Neubauer, P. (2003). A role for bacteriophage T4 rI gene function in the control of phage development during pseudolysogeny and in slowly growing host cells. Res. Microbiol. *154*, 547–552.

Lyons, N.A., Kraigher, B., Stefanic, P., Mandic-Mulec, I., and Kolter, R. (2016). A Combinatorial Kin Discrimination System in *Bacillus subtilis*. Curr. Biol. *26*, 733–742.

Maisonneuve, E., Shakespeare, L.J., Jørgensen, M.G., and Gerdes, K. (2011). Bacterial persistence by RNA endonucleases. Proc. Natl. Acad. Sci. USA *108*, 13206–13211.

Ogura, Y., Mondal, S.I., Islam, M.R., Mako, T., Arisawa, K., Katsura, K., Ooka, T., Gotoh, Y., Murase, K., Ohnishi, M., and Hayashi, T. (2015). The Shiga toxin 2 production level in enterohemorrhagic *Escherichia coli* O157:H7 is correlated with the subtypes of toxin-encoding phage. Sci. Rep. *5*, 16663.

Petrova, O.E., and Sauer, K. (2016). Escaping the biofilm in more than one way: desorption, detachment or dispersion. Curr. Opin. Microbiol. *30*, 67–78.

Ptashne, M., Backman, K., Humayun, M.Z., Jeffrey, A., Maurer, R., Meyer, B., and Sauer, R.T. (1976). Autoregulation and function of a repressor in bacteriophage lambda. Science *194*, 156–161.

Roberts, M.D., Martin, N.L., and Kropinski, A.M. (2004). The genome and proteome of coliphage T1. Virology *318*, 245–266.

Rudd, K.E. (1999). Novel intergenic repeats of *Escherichia coli* K-12. Res. Microbiol. *150*, 653–664.

Sambrook, J., Frisch, E.F., and Maniatis, T. (1989). Molecular Cloning: A Laboratory Manual, Second Edition (Cold Spring Harbor Laboratory Press).

Sternberg, N., and Coulby, J. (1990). Cleavage of the bacteriophage P1 packaging site (pac) is regulated by adenine methylation. Proc. Natl. Acad. Sci. USA *87*, 8070–8074.

Strassmann, J.E., Gilbert, O.M., and Queller, D.C. (2011). Kin discrimination and cooperation in microbes. Annu. Rev. Microbiol. *65*, 349–367.

Strockbine, N.A., Marques, L.R., Newland, J.W., Smith, H.W., Holmes, R.K., and O'Brien, A.D. (1986). Two toxin-converting phages from *Escherichia coli* O157:H7 strain 933 encode antigenically distinct toxins with similar biologic activities. Infect. Immun. *53*, 135–140.

Thieffry, D., and Thomas, R. (1995). Dynamical behaviour of biological regulatory networks–II. Immunity control in bacteriophage lambda. Bull. Math. Biol. *57*, 277–297.

Troselj, V., Cao, P., and Wall, D. (2018). Cell-cell recognition and social networking in bacteria. Environ. Microbiol. *20*, 923–933.

Tyler, A.D., Mataseje, L., Urfano, C.J., Schmidt, L., Antonation, K.S., Mulvey, M.R., and Corbett, C.R. (2018). Evaluation of Oxford Nanopore's MinION Sequencing Device for Microbial Whole Genome Sequencing Applications. Sci. Rep. *8*, 10931.

Wall, D. (2016). Kin Recognition in Bacteria. Annu. Rev. Microbiol. *70*, 143–160.

Wang, X., Kim, Y., and Wood, T.K. (2009). Control and benefits of CP4-57 prophage excision in *Escherichia coli* biofilms. ISME J. *3*, 1164–1179.

Wang, X., Kim, Y., Ma, Q., Hong, S.H., Pokusaeva, K., Sturino, J.M., and Wood, T.K. (2010). Cryptic prophages help bacteria cope with adverse environments. Nat. Commun. *1*, 147.

Webb, J.S., Lau, M., and Kjelleberg, S. (2004). Bacteriophage and phenotypic variation in *Pseudomonas aeruginosa* biofilm development. J. Bacteriol. *186*, 8066–8073.

Wood, T.K., González Barrios, A.F., Herzberg, M., and Lee, J. (2006). Motility influences biofilm architecture in *Escherichia coli*. Appl. Microbiol. Biotechnol. *72*, 361–367.

STAR★METHODS

KEY RESOURCES TABLE

REAGENT or RESOURCE	SOURCE	IDENTIFIER
Bacterial Strains and Virus		
MG1655	F. Blattner	N/A
MG1655 Δ10TA	Maisonneuve et al., 2011	N/A
MG1655 λ+	lab stock	N/A
BW25113 λ+	lab stock	N/A
O157:H7 EDL933	Strockbine et al., 1986	N/A
ATCC11303	ATCC	ATCC11303
ATCC25404	ATCC	ATCC25404
BW25113	Coli Genetic Stock Center	N/A
BW25113 (SW1): Wild type including SW1 phage	Baba et al., 2006	Keio library
yahO: BW25113 Δ*yahO* ΩKm^R	Baba et al., 2006	Keio library
nikR: BW25113 Δ*nikR* ΩKm^R	Baba et al., 2006	Keio library
yghG: BW25113 Δ*yghG* ΩKm^R	Baba et al., 2006	Keio library
rpoC: BW25113 Δ*rpoC* ΩKm^R	Baba et al., 2006	Keio library
insQ: BW25113 Δ*insQ* ΩKm^R	Baba et al., 2006	Keio library
yecA: BW25113 *A* Δ*yecA* ΩKm^R	Baba et al., 2006	Keio library
appY: BW25113 Δ*appY* ΩKm^R	Baba et al., 2006	Keio library
yfdC: BW25113 Δ*yfdC* ΩKm^R	Baba et al., 2006	Keio library
ygeA: BW25113 Δ*ygeA* ΩKm^R	Baba et al., 2006	Keio library
mhpA: BW25113 Δ*mhpA* ΩKm^R	Baba et al., 2006	Keio library
rep: BW25113 Δ*rep* ΩKm^R	Baba et al., 2006	Keio library
fhuA: BW25113 Δ*fhuA* ΩKm^R	Baba et al., 2006	Keio library
tonB: BW25113 Δ*tonB* ΩKm^R	Baba et al., 2006	Keio library
yfdR: BW25113 Δ*yfdR* ΩKm^R	Baba et al., 2006	Keio library
yfdG: BW25113 Δ*yfdG* ΩKm^R	Baba et al., 2006	Keio library
yfdL: BW25113 Δ*yfdL* ΩKm^R	Baba et al., 2006	Keio library
intS: BW25113 Δ*intS* ΩKm^R	Baba et al., 2006	Keio library
yfdQ: BW25113 Δ*yfdQ* ΩKm^R	Baba et al., 2006	Keio library
yfdS: BW25113 Δ*yfdS* ΩKm^R	Baba et al., 2006	Keio library
yfdM: BW25113 Δ*yfdM* ΩKm^R	Baba et al., 2006	Keio library
yfdI: BW25113 Δ*yfdI* ΩKm^R	Baba et al., 2006	Keio library
yfdR: BW25113 Δ*yfdR* ΩKm^R	Baba et al., 2006	Keio library
lamB: BW25113 Δ*lamB* ΩKm^R	Baba et al., 2006	Keio library
ΔCP4-57: BW25113 ΔCP4-57	Wang et al., 2010	N/A
Δrac: BW25113 Δrac	Wang et al., 2010	N/A
Δe14: BW25113 Δe14	Wang et al., 2010	N/A
ΔCPS-53: BW25113 ΔCPS-53	Wang et al., 2010	N/A
ΔCP4-6: BW25113 ΔCP4-6	Wang et al., 2010	N/A
ΔDLP12: BW25113 ΔDLP12	Wang et al., 2010	N/A
ΔQin: BW25113 ΔQin	Wang et al., 2010	N/A
ΔCP4-44: BW25113 ΔCP4-44	Wang et al., 2010	N/A
ΔCPZ-55: BW25113 ΔCPZ-55	Wang et al., 2010	N/A
Δ9: BW25113 ΔCP4-57 Δrac Δe14 ΔCPS-53 ΔCP4-6 ΔDLP12 ΔQin ΔCP4-44 ΔCPZ55	Wang et al., 2010	N/A

(*Continued on next page*)

Continued

REAGENT or RESOURCE	SOURCE	IDENTIFIER
Chemicals, Peptides, and Recombinant Proteins		
Kanamycin	Fisher Scientific	BP9065
Chloramphenicol	Fisher	BP904-100
Erythromycin	Fisher	BP920-25
Isopropyl β-D-1-thiogalactopyranoside (IPTG)	Fisher	BP1755-1
Critical Commercial Assays		
LIVE/DEAD BacLight Bacterial Viability Kit L7012	Thermo Fisher Scientific	L7012
Phage DNA isolation kit	Norgen Biotetek Corp	cat# 46800
Deposited Data		
SW1 genome sequence	This study	GenBank: PRJNA498536
Oligonucleotides		
See Table S1 for primers used in this study		
Recombinant DNA		
Plasmid: pCA24N: Cm^R; $lacI^q$	Kitagawa et al., 2005	ASKA library
Plasmid: pCA24N-yfdM: Cm^R; $lacI^q$,$P_{T5\text{-}lac}$::*yfdM*$^+$	Kitagawa et al., 2005	ASKA library
Plasmid: pCA24N-yfdQ: Cm^R; $lacI^q$,$P_{T5\text{-}lac}$::*yfdQ*$^+$	Kitagawa et al., 2005	ASKA library
Plasmid: pCM18: Em^R; P_{CP25}::gfp^+	Hansen et al., 2001	ASKA library
Plasmid: pCM18-rfp: Em^R; P_{CP25}::gfp^+-rfp^+	Hong et al., 2012	ASKA library
Software and Algorithms		
MinKNOW 2.1 software (v18.05.5, ONT)	Tyler et al., 2018	N/A
ImageJ	National Institutes of Health	https://imagej.nih.gov/ij/

CONTACT FOR REAGENT AND RESOURCE SHARING

Further information and requests for resources and reagents should be directed to and will be fulfilled by the Lead Contact, Thomas K. Wood (twood@engr.psu.edu).

EXPERIMENTAL MODEL AND SUBJECT DETAILS

The species and plasmids used in this study are listed in Table S1. For deleting and overexpressing genes, we used the Keio collection and the ASKA library. All experiments were conducted at 37°C, and cells were routinely cultured in lysogeny broth (LB) (Sambrook et al., 1989). Kanamycin (50 μg/mL) was used for pre-culturing the isogenic knockout mutants, chloramphenicol (30 μg/mL) was used for maintaining the pCA24N-based plasmids, and erythromycin (300 μg/mL) was used for maintaining the pCM18-based plasmids.

METHOD DETAILS

Motility halo assay

Swimming motility was examined using 0.3% agar plates with 1% tryptone and 0.5% NaCl. Motility and demarcation lines were analyzed after 24 h. Three plates were tested for each culture, and two independent cultures were used. Cultures (5 μL) were dropped on motility agar plates and each plate contains two strains for observing demarcation line formation and one strain for observing colony lysis zone formation; plates were incubated 16 h to form motility halos. YfdM was produced via pCA24N-yfdM via its leaky promoter or via 0.5 mM isopropyl β-D-1-thiogalactopyranoside (IPTG) as indicated. The motility agar plates were dried for 2 h to achieve consistent results.

Screening via the pooled Keio collection

To identify which *E. coli* BW25113 proteins are related to the demarcation line with MG1655, we inoculated the pooled Keio collection onto LB agar plates with kanamycin (50 μg/mL). After incubating at 37°C for 16 h, one colony from the Keio collection was inoculated with MG1655 on the same motility plate; colonies that merged with the MG1655 halo were selected, and the candidates were sequenced with primer KFp1 (Table S1). The first PCR was performed with primer Arb1 and Inv-2 with 94°C for 5 min, (94°C for 30 s, 30°C for 30 s, 72°C for 1 min)*5 cycles, (94°C for 30 s, 52°C for 30 s, 72°C for 1 min)*30 cycles, and 72°C for 5 min. The second

PCR reaction was performed with the PCR product from the first PCR reaction with primers (Arb2 and Kfp-1) using the conditions: (94°C for 30 s, 50°C for 30 s, 72°C for 1 min) *30 cycles.

To identify which proteins are required for SW1 phage infection in BW25113, SW1 phage stock (10^{11} pfu/mL) was added (10%) to the pooled Keio culture with a turbidity of 1.0 at 600 nm. The culture was spread on LB agar plates with kanamycin when the culture reached a turbidity of 0.1 at OD 600, and the DNA from the colonies was sequenced.

Gel pad microscopy with GFP/RFP-labeled strains

The GFP/RFP labeled strains were inoculated on motility agar on glass slides and incubated overnight. The motility agar was covered with a cover glass, and the fluorescence signal was analyzed by microscopy (Zeiss Axioscope.A1) using excitation at 488 nm and emission at 500 nm for GFP fluorescence and using excitation at 561 nm and emission at 575 nm for RFP fluorescence.

Plaque assay

Supernatants from the strains were harvested by centrifugation (8000 *g* for 10 min) and filtered (0.2 μm), then phage was quantified by counting plaques using a modified top-layer agar method (Eisenstark, 1967). The plaque assay was performed with three independent cultures for each strain with three replicates for each culture. EHEC phage were induced by mitomycin C (10 μg/mL) for obtaining EHEC phage.

Polymerase chain reaction (PCR) to detect phages

To detect lambda phage and ϕ80, PCR was performed with a colony that was mixed with 20 μL of water and boiled for 10 min; 2 μL of the crude cell extract was used with primers shown in Table S1. To detect phage genes in SW1, phage DNA was used as the DNA template with primers shown in Table S1 after isolating the phage DNA by the Phage DNA isolation kit 46800 (Norgen Biotetek Corp). To detect SW1 phage genes associated with BW25113 (SW1) and BW25113 (SW1)/pCA24N-yfdM, genomic DNA was used for BW25113 (SW1) and a culture (i.e., cells + supernatant) of BW25113 (SW1)/pCA24N-yfdM was used as the DNA template with primers shown in Table S1.

Electron microscopy

For transmission electron microscopy (TEM), the BW25113/pCA24N-YfdM culture was cultured for 48 h to lyse cells, centrifuged at 8000 *g*, and the supernatant was filter-sterilized (0.2 μm). The samples were fixed with buffer (2.5% glutaraldehyde in 0.1M cacodylate buffer, pH 7.4) and negative stained with 2% uranyl acetate in the dark for 1 h, then dehydrated. The sectioned specimens were stained again with uranyl acetate and lead citrate after dehydration, resin embedding, and the sectioning process. TEM images were obtained using a JEOL JEM 1200 EXII instrument. For scanning electron microscopy (SEM), the samples were collected at 0 h, 3 h, and 6 h after adding the phage stocks to BW25113 cells. The sample was fixed with buffer (2.5% glutaraldehyde in 0.1M cacodylate buffer, pH 7.4). SEM images were obtained using a Zeiss SIGMA VP-FESEM instrument.

Viability assay

Once the demarcation line between the strains was formed, it was removed from the motility agar and stained for 1 h at room temperature in the dark using the using the LIVE/DEAD BacLight Bacterial Viability Kit L7012 (Molecular Probes, Inc., Eugene, OR). The fluorescence signal was analyzed via microscopy using excitation at 485 nm and emission at 530 nm for green fluorescence and using excitation at 485 nm and emission at 630 nm for red fluorescence (Zeiss Axioscope.A1).

Infection with SW1 phage

To infect bacteria with SW1 phage, phage stock (2% by vol) was added to a culture when the strain reached a turbidity of 1.0 at 600 nm and it was incubated for 24 h.

Infection with lambda phage

To infect bacteria with lambda phage, phage stock (2% by vol) was added to a culture when the strain reached a turbidity of 0.8 at 600 nm, and it was incubated for 6 h. The lambda phage stock was made by inducing MG1655 (λ) with mitomycin C (1 μg/mL) and filtering (0.2 μm).

Phage DNA genome sequencing

Phage DNA was isolated from BW25113/pCA24N-YfdM after growth in LB for 36 h by the Phage DNA isolation kit (Harrison et al., 2009; 46800, Norgen Biotetek Corp). The DNA library was prepared using a Ligation Sequencing Kit (SQK-LSK108, ONT). Briefly, 1.5 μg of phage genomic DNA in 50 μL distilled water were fragmented by g-TUBE (Harrison et al., 520079, Covaris), and the DNA fragments were end-repaired and ligated to sequencing adapters. The sequencing was performed with a MiniON flowcell (MIN-106) (achieves 97% accuracy with 40X coverage) (Tyler et al., 2018) and MinKNOW 2.1 software (v18.05.5, ONT) for 24 hours and generated about 1,416,720 reads (fast5 files). Albarcore (v2.3.1, ONT) was used for base calling, and about 10.03 Gb were obtained. Since the genome size of SW1 is approximate 50 kb, only 4 fastq files containing 16,000 reads (98,124,380 bp) were used for *de novo* assembly via Canu (v1.6) for 2,000X coverage. For polishing and higher accuracy, contigs were subsequently processed with

Racon (v1.3.1) and Miniasm-0.3 (r179). Using Circlator (v1.5.1), a single circular phage genome was generated (49,245 bp). Genome annotation was performed by Phast server (http://phast.wishartlab.com).

QUANTIFICATION AND STATISTICAL ANALYSIS

Scoring via the demarcation line index (DLI)

The DLI is the combined scores for demarcation line darkness (color), gap width, and consistency (extent over the intersection) between two competing halos inspired by the scoring method for disease activity which characterizes the clinical and histopathology features of the dextran sulfate sodium mouse model (Cooper et al., 1993). The maximum DLI score is 10 and scores $\geq$ 4 indicate the presence of a clear demarcation line (indicated by a red arrow), and DLI scores $\leq$ 3 indicate motility halo merging (indicated by a green arrow). The specific metrics used are shown in the following table:

Score	Color(darkness)	Gap	Consistency of DL
0	none	none	none
1	different halo color but no gap	thin gap (+)	showing partial DL and partial merging
2	gray	gap (++)	showing consistent of DL (color, gap)
3	dark gray	thicker gap (+++)	-
4	black	thick gap (++++)	-

A score of 4 was chosen as the cutoff since samples that had this score had the basic attributes of a clearance zone between the two motility halos. Each condition was evaluated for a DLI with at least two independent cultures and two replicates for each independent culture so a minimum of 4 motility plates were used (many samples had more plates than this).

Statistical analysis

All results are presented as the mean ± SEM. Microsoft Excel and Sigma Plot Statistics were used for statistical analysis. Data were analyzed using one-way ANOVA as specified in the Figure legends. ** ($p < 0.01$) indicates significant differences between BW25113 and BW25113 (SW1).

DATA AND SOFTWARE AVAILABILITY

The accession number for the SW1 phage sequence reported in this paper is GenBank: PRJNA498536.